HYCELL-A new hybrid model of the rain horizontal distribution for propagation studies: 2. Statistical modeling of the rain rate field

Laurent Féral, Henri Sauvageot, Laurent Castanet, Joël Lemorton

RADIO SCIENCE, VOL. 38, NO. 3, 1057, doi:10.1029/2002RS002803, 2003

HYCELL—A new hybrid model of the rain horizontal distribution for propagation studies: 2. Statistical modeling of the rain rate field

Laurent Féral

Département Electromagnétisme et Radar, Office National d'Etudes et de Recherches Aérospatiales, Toulouse, France

Henri Sauvageot

Observatoire Midi-Pyrénées, Laboratoire d'Aérologie, Université Paul Sabatier, Toulouse, France

Laurent Castanet and Joël Lemorton

Département Electromagnétisme et Radar, Office National d'Etudes et de Recherches Aérospatiales, Toulouse, France

Received 24 October 2002; revised 24 February 2003; accepted 28 March 2003; published 13 June 2003.

[1] A methodology to simulate typical two-dimensional rain rate fields over an observation area A_o of a few tens up to a few hundreds of square kilometers (i.e., the scale of a satellite telecommunication beam or a terrestrial Broadband Wireless Access network) is proposed. The scenes generated account for the climatological characteristics intrinsic to the simulation area A_o. The methodology consists of the conglomeration of rain cells modeled by HYCELL and of two analytical expressions of the rain cell spatial density, both derived from the statistical distribution of the rain cell size. The scene generating requires, as an input parameter, the local Cumulative Distribution Function (CDF) of the rain rate, a meteorological data commonly available throughout the world. The rain rate field is then generated numerically, according to an iterative scheme, under the constraint of accurately reproducing the local CDF intrinsic to the simulation area A_o, and following rigorously the rain cell spatial density. All the potentialities of the HYCELL model are thus used in order to generate a two-dimensional scene having a mixed composition of hybrid, gaussian, and exponential cells accounting for the local climatological characteristics. Various scenes are then simulated throughout the world, showing the ability of the method to reproduce the local CDF, with a mean error, with respect to the rain rate distribution, smaller than 1.86%, whatever the location, that is, whatever the climatology. It is suggested that this statistical modeling of the rain rate field horizontal structure be used as a tool by system designers to evaluate, at any location of the world, diversity gain, terrestrial path attenuation, or slant path attenuation for different azimuth and elevation angle directions. *INDEX TERMS:* 3354 Meteorology and Atmospheric Dynamics: Precipitation (1854); 3210 Mathematical Geophysics: Modeling; 3360 Meteorology and Atmospheric Dynamics: Remote sensing; 6964 Radio Science: Radio wave propagation; *KEYWORDS:* propagation in rain, radar meteorology, rain modeling

Citation: Féral, L., H. Sauvageot, L. Castanet, and J. Lemorton, HYCELL—A new hybrid model of the rain horizontal distribution for propagation studies: 2. Statistical modeling of the rain rate field, *Radio Sci.*, *38*(3), 1057, doi:10.1029/2002RS002803, 2003.

1. Introduction

[2] Because of congestion at conventional frequency bands (L, S, C, and Ku), and users' increasing needs to convey higher data rates, the evolution of satellite telecommunications requires use of frequency bands higher than 20 GHz. This frequency shift raises problems related to the influence of atmospheric precipitation on electromagnetic propagation [*Castanet et al.*, 2001; *Lemorton et al.*, 2001]. Fade Mitigation Techniques (FMT) such as power control, adaptive waveform, or

0048-6604/03/2002RS002803

site diversity have to be implemented [*Castanet et al.*, 2002a].

[3] In other respects, telecommunication systems under consideration at Ka and V-bands for multimedia applications, are based on a regional covering composed of a set of contiguous beams [*Pech et al.*, 2002]. In the first generation system, they will be regularly distributed and fixed. In a second generation using active antennas, the beams should be flexible [*Castanet et al.*, 1998], depending on the required traffic and the propagation conditions. Consequently, system designers have to evaluate the impact of precipitation not on a particular link but at the scale of one or several beams [*Castanet et al.*, 2002b]. This is also the case for the terrestrial Broadband Wireless Access network (BWA) at 28 or 42 GHz, where the presence of rain on a cell or a cluster of cells affects the availability, the interference, and the capacity performance of the network.

[4] In this context, the simulation of a typical two-dimensional rain rate field over an area of a few tens up to a few hundreds of square kilometers (terrestrial network, satellite telecommunication beam), whose properties are in accordance with the local climatology, would be a powerful tool for system designers to evaluate, at any location, diversity gain, terrestrial or slant path attenuation for different azimuth directions [*Bolea-Alamanac and Bousquet*, 2002; *Riva*, 2002].

[5] Two-dimensional rain rate fields are precisely the kind of information that is provided by meteorological radars, in the form of Constant Altitude Plan Position Indicator (CAPPI), giving the almost instantaneous spatial distribution of the rain rate over an observation area A_o. Unfortunately, few regions in the world are equipped with meteorological radars properly operated for long periods. Models, therefore, have to be developed in order to provide the required data.

[6] Fortunately, one of the most common meteorological parameters available throughout the world is the rain rate cumulative distribution function (CDF) [*Poiares-Baptista and Salonen*, 1998]. Due to its statistical nature, the CDF accounts for the average climatological characteristics of the geographic location it refers to. However, how is it possible to generate a rain rate field over an observation area A_o so that the simulated scene should account for the local climatology, that is, for the local CDF?

[7] As it is difficult to describe and, a fortiori, to model a rain rate field by considering it as a single entity, it might be possible to split up the field into individual areas, the rain cells, defined as the closed contours over which the rain rate R exceeds a threshold value τ. This cellular approach is all the more interesting as deterministic models of rain cells are available, allowing one to describe the inner structure of the cells from a small number of parameters, such as those proposed by *Capsoni et al.* [1987b] or *Féral et al.* [2003]. Whatever the model considered, the two-dimensional generation of a rain rate field from modeled cells requires the determination of a key parameter: the spatial density of the cells, expressed as a function of the model parameters. Of course, this density can only be statistical in nature and may display significant differences from the climatology of the location it refers to.

[8] *Goldhirsh* [2000] proposed a method for simulating typical two-dimensional rain rate fields, at any particular geographic location, from the CDF intrinsic to the region considered. The method relies on the rain cell modeling by EXCELL [*Capsoni et al.*, 1987a, 1987b] and allows one to fill in the observation area A_o with a population of cells having exponential profiles and rotational symmetry. To determine the rain cell spatial density over A_o, *Goldhirsh* [2000] uses the analytic formulation of *Capsoni et al.* [1987b], slightly corrected by *Awaka* [1989]. The cell density involves the EXCELL parameters and the local CDF intrinsic to the simulation area A_o.

[9] This methodology leads to some remarks. First, HYCELL [*Féral et al.*, 2003] now provides a new model of the rain cell which describes the rain cell horizontal structure more accurately than EXCELL. Secondly, the analytical expression of the cell spatial density has been derived by *Capsoni et al.* [1987b] from the radar observation of 6215 cells in the region of Milan (Italy, midlatitude area). Hence the question: "can the same expression of cell spatial density be used when generating, for instance, a rain field in tropical regions?" Third, as will be shown in the present paper, the scene finally generated does not accurately follow the local CDF given as an input parameter.

[10] The object of this paper is to propose a new methodology for generating, over an observation area A_o, a two-dimensional rain rate field composed of hybrid cells, that is to say modeled by HYCELL [*Féral et al.*, 2003], so that the simulated scene accounts for the climatological characteristics of the simulation area A_o. The mathematical definition of the HYCELL model is reviewed in Section 2. In Section 3, from the distribution of rain cell diameters (a statistical distribution widely studied in the literature in various climates), two analytical expressions of the cell spatial density are derived, both involving the local CDF. A methodology is then presented in Section 4 for the numerical generation of a rain rate field over an observation area A_o so that the generated scene accurately follows the CDF characteristic of the simulation area A_o. Some examples of simulated rain rate fields in various latitudes are then given. Finally, comparative results are presented in Section 5, showing the ability of the methodology to simulate

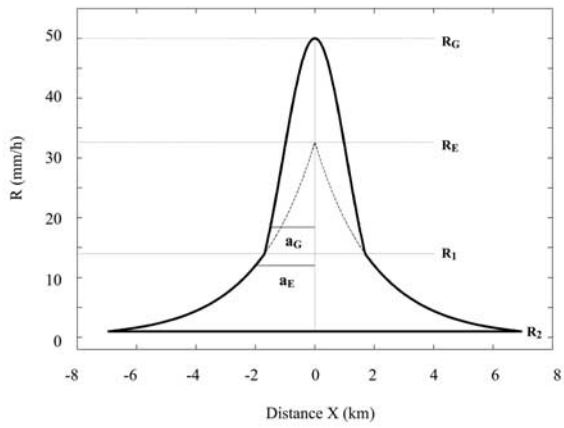

Figure 1. Representation in the vertical plane passing through the (Ox) axis of the HYCELL modeling. R_G and R_E are the gaussian and the exponential peaks, respectively. a_G and a_E are the distances for which the rain rate R decreases by a factor 1/e with respect to R_G and R_E, respectively. R_1 delimits the zones of gaussian and exponential definition. $R_2 = 1$ mm h^{-1}.

typical two-dimensional rain rate fields accounting for the local CDF.

2. Rain Cell Modeling

[11] As mentioned in the previous section, the rain cells are defined as the area inside which the rain rate $R \geq \tau$ [e.g., *Drufuca*, 1977; *Goldhirsh and Musiani*, 1986]. The cell is continuous and, along the contour that bounds it, the rain rate is equal to the threshold value τ.

2.1. Hybrid Modeling of the Rain Cell Horizontal Structure: The HYCELL Model

[12] *Féral et al.* [2003] proposed to describe the rain rate horizontal distribution (RRHD) within rain cells having an elliptic horizontal cross section by combining a gaussian component with an exponential one (Figure 1), so that the analytical expression of the RRHD becomes, in the horizontal plane (Oxy):

$$\left.\begin{aligned} R(x,y) &= R_G \exp\left[-\left(\frac{x^2}{a_G^2}+\frac{y^2}{b_G^2}\right)\right] \text{if } R \geq R_1 \\ &= R_E \exp\left[-\left(\frac{x^2}{a_E^2}+\frac{y^2}{b_E^2}\right)^{1/2}\right] \text{if } R_2 \leq R < R_1 \end{aligned}\right\} \quad (1)$$

R_G, a_G, and b_G define the gaussian component and are the peak rain rate and the distances along the (Ox) and (Oy) axes for which the rain rate decreases by a factor 1/e with respect to R_G, respectively. R_E, a_E, and b_E define the exponential component with similar signification as for the gaussian component as shown in Figure 1 where the hybrid modeling parameters are represented in a vertical plane passing by the Ox axis. R_1 separates the gaussian and exponential components. From *Féral et al.* [2003], the domain of definition of HYCELL is $R \geq R_2$, with $R_2 = 1$ mm h^{-1}.

[13] The HYCELL model was validated from radar observations of rain rate fields. Considering a database of 213 112 rain cells identified at $\tau = R_2 = 1$ mm h^{-1} from the radar of Météo-France at Bordeaux in 1996 (southwestern France, midlatitude oceanic climate), and another database composed of 701 882 cells observed at the same threshold from the radar of Karlsruhe in 1999 (southwestern Germany, midlatitude continental climate), *Féral et al.* [2003] have shown that, whatever the climatology, the HYCELL model enables one to improve the description of the rain rate horizontal distribution within the cells with respect to the well-known EXCELL model [*Capsoni et al.*, 1987b].

[14] From (1), the HYCELL modeling of a rain cell requires the determination of seven parameters (R_G, a_G, b_G, R_E, a_E, b_E, and R_1). They are obtained, cell by cell, by forcing some parameters of integral nature to be the same for the measured radar cells as for the modeled cells [*Féral et al.*, 2003]. Depending on the value of R_1, HYCELL is able to generate purely exponential ($R_1 = R_E = R_G$), purely gaussian ($R_1 = R_2$), and hybrid cells ($R_2 < R_1 < R_G$). For the latter, one can wonder whether a statistical relationship between R_G and R_1 exists. To answer this question, from the databases of Bordeaux and Karlsruhe, the conditional mean of R_1 given R_G and the conditional standard deviation of R_1 given R_G were determined either by considering classes of R_G or using kernel method [*Silverman*, 1996]. Both techniques lead to the same conclusion. Figures 2 and 3 show the results derived from the modeled cells of Bordeaux and Karlsruhe, respectively. The regression lines were obtained by least squares fitting with the additional constraint of zero intercept. From these two figures, it is clear that the conditional mean value of R_1 is close to 0.55 R_G while the conditional standard deviation of R_1 is close to 0.20 R_G. Consequently, the conditional mean values of R_1 are tainted with high variances which reflect the strong variabilities of rain cell horizontal structure. Now, as part of the statistical modeling of rain rate fields and as will be shown latter in the paper, the value of R_1 will be iteratively corrected, from its average value 0.55 R_G down to $R_2 = 1$ mm h^{-1} accounting, to a certain extent, for the variabilities of parameter R_1. Though the statistical analysis of the marginal distributions of the HYCELL model parameters could prove very interest-

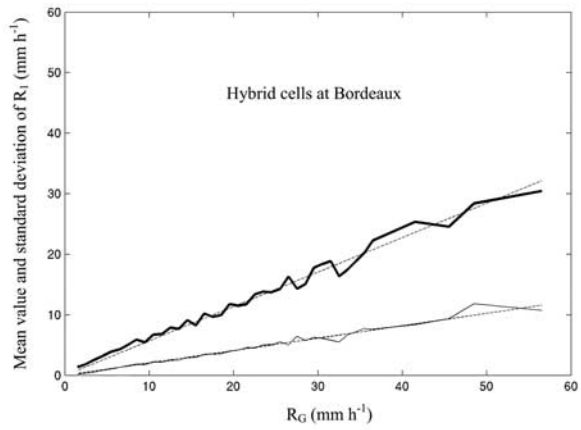

Figure 2. Mean value (bold solid line) and standard deviation (solid line) of R_1 as a function of R_G for the hybrid cells ($R_2 < R_1 < R_G$), modeled from the radar observations at Bordeaux. The regression lines (dotted) are obtained by least squares fitting with the additional constraint of zero intercept. Their equations are $R_1 = 0.569\ R_G$ with a correlation coefficient ρ of 0.99 and $R_1 = 0.205\ R_G$ ($\rho = 0.99$) for mean and standard deviation, respectively.

ing, it is not developed here insofar as it is out the scope of the present paper.

2.2. Distribution of the Rain Cell Diameter

[15] Many authors [*Dennis and Fernald*, 1963; *Miller et al.*, 1975; *Konrad*, 1978; *Goldhirsh and Musiani*, 1986; *Tenorio et al.*, 1995; *Sauvageot et al.*, 1999; *Mesnard and Sauvageot*, 2003] have considered that rain cells can be approximated by a circular shape. The diameter of the circular cell of equivalent area is used as a characteristic measure of the rain cell size. Most authors have proposed an exponential form to represent the rain cell size distribution (RCSD); that is:

$$N(D,\tau) = N_o(\tau)\exp[-\lambda(\tau)D] \qquad (2)$$

where D is the diameter of the circular cell of equivalent area over which the rain rate R is above the threshold τ; $N(D, \tau)$ is the number of cells having a diameter D at τ, per unit area inside an observed area A_o; $N_o(\tau)$ and $\lambda(\tau)$ are the two parameters of the distribution, that is the intercept and the slope, respectively. Obviously, $N(D, \tau)$ is a conditional distribution insofar as the necessary condition to observe $R \geq \tau$ is that it should be raining. So $N(D, \tau)$ is understood as the diameter distribution, given that it is raining over A_o.

[16] From Table 1, which sums up chronologically the main results related to RCSD, it appears that λ is not only weakly dependent on the threshold but also weakly variable from one place to another. The excessive large values found by *Goldhirsh and Musiani* [1986] probably result from the small maximum diameter D_{max} considered in the regressions (only 5 km). Indeed, λ tends to increase as D_{max} decreases. Moreover, Table 1 shows that the maximum size considered for the rain cells is about 20 km in equivalent diameter (314 km^2 in area). This right truncation is justified by the fact that rain structures larger than about 300 km^2 are no longer rain cells but rather cell clusters controlled by air motions of scale larger than the rain cell. Therefore, for D lying between 2 and 20 km, Table 1 leads to the conclusion that λ can be considered as a climatic constant whose value is around 0.30 km^{-1}.

[17] The next question is whether the RCSD is well represented by (2) for diameters below 2 km. *Mesnard and Sauvageot* [2003] answered this question and showed that the RCSD is in fact best fitted by a lognormal function, whose modal value is less than about 2 km, that is located at a diameter smaller than the minimum size that can be resolved by most of the radars at the farthest part of their observation area. In such a way, (2) corresponds to the analytical fitting of a (lognormal) distribution truncated on the left, at size larger than the modal value, so that the validity domain of (2) has to be restrained to the diameter interval 2 km $\leq$ D $\leq$ 20 km.

[18] Now, when considering rain cells of circular horizontal cross section, the HYCELL modeling of a cell requires the determination of five parameters, namely R_G, a_G, R_E, a_E, and R_1 insofar as $b_G = a_G$ and

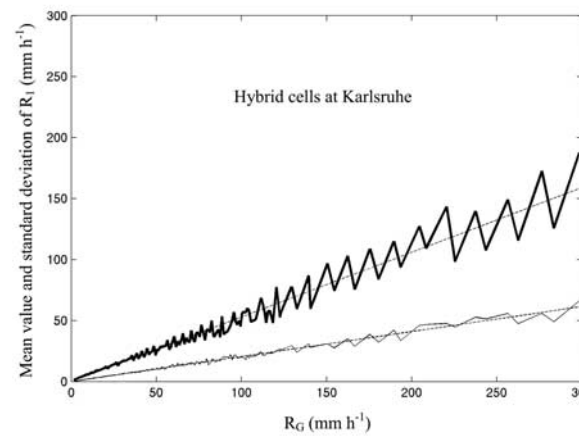

Figure 3. Same as Figure 2 but now from the radar observations at Karlsruhe. The equations of the regression lines (dotted) are $R_1 = 0.53\ R_G$ ($\rho = 0.97$) and $R_1 = 0.205\ R_G$ ($\rho = 0.99$) for mean and standard deviation, respectively.

Table 1. Summary of Experiments and Results on the Rain Cell Diameter Distribution[a]

Reference	Location	Season or Date	Observational Technique	Radar Beam Width θ	Range of D (km) Considered for RCSD Computation		Threshold τ, mm h^{-1}	λ, km^{-1}	Correlation Coefficient
					D_{min}	D_{max}			
Dennis and Fernald [1963]	England 53°N	Spring	Radar	NS	NS	NS	Noise level	0.22	NS
	Illinois 40°N,88°E	Spring		NS	NS	NS	Noise level	0.30	NS
	Picket ship:								
	49°N,131°W	Entire year		NS	NS	NS	Noise level	0.27	NS
	45°N,130°W	Entire year		NS	NS	NS	Noise level	0.24 and 0.32	NS
	40°N,130°W	Entire year		NS	NS	NS	Noise level	0.35	NS
	36°N,128°W	Entire year		NS	NS	NS	Noise level	0.38	NS
	32°N,124°W	Entire year		NS	NS	NS	Noise level	0.38	NS
	Eniwetok Atoll	5-12 April 1960	3-cm radar	1°	~2	20	Noise level	0.38	0.99
Miller et al. [1975]	North Dakota 43°N,104°E	Summer 1972	10-cm radar	NS	2	15	Noise level	0.35	0.97
Konrad [1978]	Wallops Island, Virginia 38°N,75°E	May-August 1973	10-cm radar	~0.44°	2	14	~0.15	0.36	NS
				horizontal	2	14	2.7–5.6 to 100–205	0.42–0.50	NS
Goldhirsh and Musiani [1986]	Wallops Island, Virginia 38°N,75°E	17 days over 5 years, all seasons	10-cm radar	~0.44°	1	5	15 intervals between 0.5 to >205 mm h^{-1}	0.79	0.98
Tenorio et al. [1995]	Niamey 13°N,2°E	Rainy season 1992	5-cm radar	1.4°	2	18	7 intervals between 0.13 to >55 mm h^{-1}	0.32–0.38	0.93
Mesnard and Sauvageot [2003]	Bordeaux 44°N,0.3°W	Year 1996	10-cm radar	1.75°	3	15	8 intervals between 1 to >16 mm h^{-1}	0.30–0.43	0.97
	Toulouse 43°N,1°E	September 1996	5-cm radar	1.3°	3	15		0.31–0.33	0.98
	Abidjan 5°N,4°W	Rainy season 1995 and 1996	5-cm radar	1.3°	3	15		0.29–0.38	0.97

[a]Adapted from *Sauvageot et al.* [1999]. NS, not specified.

$b_E = a_E$. Ever since, as part of a two-dimensional scene generating over an observation area A_o from a population of (circular) cells modeled by HYCELL, two questions arise. How many cells occupy A_o? How to model them? That is to say, for each cell filling A_o, which values should be given to R_G, a_G, R_E, a_E, and R_1? These questions may be addressed by the rain cell spatial density. The following section is dedicated to its analytical determination. Two expressions will be derived from the rain cell diameter distribution (2) which involve the local CDF, intrinsic to the simulation area A_o.

3. Rain Cell Spatial Density

3.1. Analytical Expressions of the Rain Cell Spatial Density

[19] Let A_o be the observation area and $A_r = \alpha A_o$ the area over which it is raining, that is over which the rain rate R is larger than a threshold R_r ($0 < \alpha \leq 1$ so that $A_r \subset A_o$). From a spatial point of view, the conditional probability that the rain rate R exceeds the value R* over A_o, given that it is raining ($R > R_r$), can be written:

$$P(R \geq R^*/R > R_r) = P_r(R^*) = \frac{A(R \geq R^*)}{A_o} \frac{A_o}{A(R > R_r)} = \frac{A(R \geq R^*)}{A_r}. \quad (3)$$

[20] For rain cells of circular shape, (2) gives the number of cells having a diameter D per unit area with respect to R*, given it is raining ($R > R_r$). Considering rain cells whose size lies between D_{min} and D_{max}, (3) can be rewritten:

$$P_r(R^*) = \int_{D_{min}}^{D_{max}} S_o(D) N(D, R^*) dD, \quad (4)$$

where $S_o(D)$ is the area of the rain cell with diameter D. As previously mentioned, the maximum diameter of a rain cell is about 20 km so that D_{max} can be replaced by ∞ with an error smaller than 6.3%. Therefore, λ being a climatic constant, using (2) in (4) results in:

$$P_r(R^*) = \int_{D_{min}}^{\infty} \pi \frac{D^2}{4} N_o(R^*) e^{-\lambda D} dD = \frac{\pi}{4} \left[\frac{D_{min}^2}{\lambda} + \frac{2D_{min}}{\lambda^2} + \frac{2}{\lambda^3} \right] e^{-\lambda D_{min}} N_o(R^*), \quad (5)$$

so that finally:

$$N_o(R^*) = \frac{4}{\pi} \left[\frac{D_{min}^2}{\lambda} + \frac{2D_{min}}{\lambda^2} + \frac{2}{\lambda^3} \right]^{-1} e^{\lambda D_{min}} P_r(R^*). \quad (6)$$

[21] The total number of cells (N_T) at R* per unit area, given that it is raining, is:

$$N_T(R^*) = \int_{D_{min}}^{\infty} N(D, R^*) dD = \frac{N_o(R^*)}{\lambda} e^{-\lambda D_{min}}. \quad (7)$$

[22] On the one hand, as part of the rain cell modeling by HYCELL, the difference between the total number of cells at R* and at R* + ΔR*, that is $N_T(R^*) - N_T(R^* + \Delta R^*)$, is the spatial density N_p of cells whose peak value R_G lies between R* and R* + ΔR* so that:

$$N_P(R_G) = N_T(R^*) - N_T(R^* + \Delta R^*) = -\frac{4}{\lambda \pi} \left[\frac{D^2_{min}}{\lambda} + \frac{2D_{min}}{\lambda^2} + \frac{2}{\lambda^3} \right]^{-1} [P_r(R^* + \Delta R^*) - P_r(R^*)], \quad (8)$$

that is:

$$N_P(R_G) = -\frac{4}{\lambda \pi} \left[\frac{D^2_{min}}{\lambda} + \frac{2D_{min}}{\lambda^2} + \frac{2}{\lambda^3} \right]^{-1} \cdot \left[\frac{d}{dR} P_r(R) \right]_{R=R_G} \Delta R_G. \quad (9)$$

A first expression of the rain cell spatial density is given by (9) as a function of the HYCELL peak rain rate R_G, the first derivative of the spatial conditional CDF, λ, and D_{min}.

[23] On the other hand, from (2), the cell spatial density N_D whose diameter lies between D and D + ΔD at R* can be derived:

$$N_D(R^*) = \int_{D}^{D+DD} N(D, R^*) dD = \frac{N_o(R^*)}{\lambda} \left[e^{-\lambda D} - e^{-\lambda (D + \Delta D)} \right] = \frac{4}{\lambda \pi} \left[\frac{D^2_{min}}{\lambda} + \frac{2D_{min}}{\lambda^2} + \frac{2}{\lambda^3} \right]^{-1} \cdot e^{\lambda D_{min}} P_r(R^*) \left[e^{-\lambda D} - e^{-\lambda (D + \Delta D)} \right], \quad (10)$$

which gives a second expression of the rain cell spatial density as a function of the rain cell diameter D, the rain rate R*, the spatial conditional CDF P_r, λ, and D_{min}.

3.2. Determination of the Spatial Conditional CDF

[24] In the above equations, the conditional probability that the rain rate may exceed the value R* over A_o given that it is raining, that is $P(R \geq R^*/R > R_r)$ or $P_r(R^*)$, may be derived from purely spatial considerations. On the other hand, the yearly average cumulative distribution of

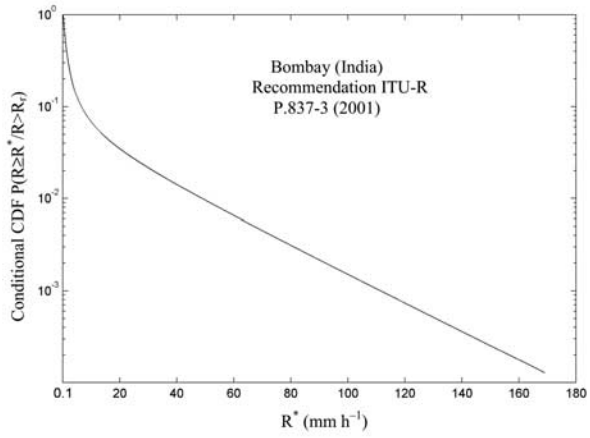

Figure 4. Conditional CDF for Bombay, India (l = 18°54′ N, L = 72°48′ E) derived from recommendation *ITU* [2001]. The threshold condition of rain is $R = R_r = 0.1$ mm h^{-1} so that for $R = R_r$, the CDF is equal to 1.

the rain rate can be calculated throughout the world using recommendation *International Telecommunication Union* (*ITU*) [2001]. This model allows the CDF of the rain rate to be calculated on a yearly basis from a cartography of radio-meteorological parameters (amount of stratiform rain, amount of convective rain, probability of rain within six hours). These worldwide maps have been obtained using the ECMWF (European Centre for Medium-Range Weather Forecasts) weather forecast model calibrated with long-term radiosondes and rain rate data. Consequently, these distributions are not derived from spatial characteristics, but rather from temporal ones.

[25] *Nzeukou and Sauvageot* [2002] have shown that the PDF of rain rate, whether it is computed from spatial (radar) or temporal (rain gauge) observations of rainy events, is lognormal so that it is fully determined by its mean μ and its standard deviation σ. Considering spatial and temporal observations of rain fields (subscript S and T, respectively), they showed that $\mu_S = \mu_T$ and $\sigma_S = \sigma_T$, leading to the conclusion that rain fields are ergodic. This property implies that the PDF of the rain rate obtained from temporal observations of rainy events is the same as the one derived from spatial observations, leading to the conclusion that the temporal CDF is also the spatial CDF.

[26] In such conditions, the spatial conditional CDF $P(R \geq R^*/R > R_r)$ can be derived from a temporal model of the rain rate CDF, such as the ones given in recommendation *ITU* [2001] which gives, for any location in the world characterized by its latitude l and its longitude L, the time percentage of an average year during which the rain rate R* is exceeded. The modeled temporal CDF has then to be turned into a conditional one. In the present paper, it will be assumed that $R_r = 0.1$ mm h^{-1} defines the threshold condition of rain previously introduced, so that the conditional CDF is defined for $R \geq R_r$ and is simply obtained by dividing the absolute CDF given by recommendation *ITU* [2001] by its value for $R = R_r = 0.1$ mm h^{-1}. Now, if meteorological radars are able to measure rain rates at 0.1 mm h^{-1}, measurements from tipping bucket rain gauge may introduce errors because of updrafts suspending small drops (i.e., they do not reach still air terminal velocity) and because evaporation is likely to occur. To overcome these points, a larger value of R_r can be selected (e.g., $R_r = 0.5$ mm h^{-1}, for example). Moreover, the availability percentage required for telecommunication systems in Ka and V-bands is about 99.99% of the average year. This would lead to focus on the values of the absolute CDF greater than 0.01%. In the present paper, this left truncation will be taken equal to 0.001%, corresponding to a system availability requirement of 99.999%. As an example, Figure 4 shows the conditional CDF obtained this way for Bombay, India (l = 18°54′ N, L = 72°48′ E).

4. Statistical Modeling of Rain Rate Fields

[27] The object of the present section is to develop a methodology enabling the generation of a rain rate field over a simulation area A_o from cells modeled by HYCELL, in such a way that the generated scene is consistent with the CDF characteristic of A_o. As the domain of definition of HYCELL is $R \geq R_2$ with $R_2 = 1$ mm h^{-1}, the contribution of the modeled cells will be limited to rain rates greater than 1 mm h^{-1}. Therefore, the simulated rain rate field over A_o is expected to reproduce the local CDF for $R \geq 1$ mm h^{-1}.

[28] Moreover, for the sake of clarity, the step by step methodology for generating a typical two-dimensional rain rate field over a simulation area A_o in the region of Bombay (l = 18°54′ N, L = 72°48′ E) is given here. The choice of Bombay is totally arbitrary and constitutes only an example. It is assumed that the observation area A_o is 100×100 km^2 and that the area over which the rain rate exceeds $R_r = 0.1$ mm h^{-1}, that is A_r, fully occupies A_o (with $A_r/A_o = \alpha = 1$). This assumption seems reasonable taking into account the low value of the threshold condition on rain R_r and the size of A_o. From the two analytical expressions of the rain cell spatial density (9) and (10), the number of hybrid cells occupying A_o, their peak value R_G and their diameter at 1 mm h^{-1} will be determined.

4.1. Determination of $(R_{G,i})_{i=1..N}$ and $(D_i)_{i=1..N}$

[29] From (9), and considering an observation area A_o over which the rain rate $R > R_r$ occupies A_r, the number

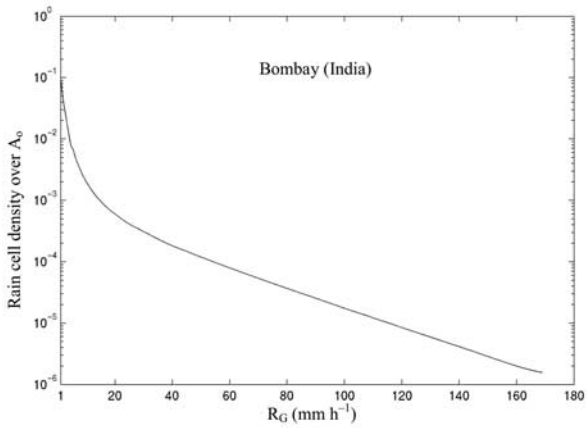

Figure 5. Rain cell density as a function of their peak R_G for Bombay, when $A_o = A_r = 100 \times 100$ km^2 ($\alpha = 1$), $D_{min} = 2$ km, $\lambda = 0.30$ km^{-1}, and $\Delta R_G = 0.001$ mm h^{-1}.

of cells n_p whose peak value is equal to R_G (i.e., the cell density per class of R_G) is given by:

$$n_P(R_G) = -\frac{4}{\lambda\pi}\left[\frac{D_{min}^2}{\lambda} + \frac{2D_{min}}{\lambda^2} + \frac{2}{\lambda^3}\right]^{-1} \cdot \left[\frac{d}{dR}P_r(R)\right]_{R=R_G} \Delta R_G A_r. \quad (11)$$

[30] As the HYCELL domain of definition is $R \geq R_2$, with $R_2 = 1$ mm h^{-1}, the peak rain rate R_G of the hybrid cells occupying A_o lies between 1 mm h^{-1} and the maximum value of R given by recommendation *ITU* [2001]. In the case of Bombay, it leads to considering R_G varying from 1 to 168.95 mm h^{-1} by ΔR_G steps. Whatever the value of A_r, the incremental step ΔR_G can always be chosen sufficiently small to insure that the number of cells per value of R_G is always smaller than one. In other words, the method results in an oversampling of R_G. This requires the determination of P_r for the successive values of R_G, which is easily done by means of a cubic spline interpolation. Figure 5 shows the cell density as a function of their peak value R_G obtained that way for Bombay, when $A_o = A_r = 100 \times 100$ km^2 ($\alpha = 1$), $D_{min} = 2$ km in compliance with the domain of definition of (2), $\lambda = 0.30$ km^{-1} and $\Delta R_G = 0.001$ mm h^{-1}.

[31] A resampling of R_G is then operated in order to have systematically one cell per value of R_G. Therefore, N hybrid cells of peak value $(R_{G,i})_{i=1..N}$ sorted in descending order ($R_{G,1} > R_{G,2} > \ldots > R_{G,N}$) occupy the observation area A_o. Proceeding that way, in the case of Bombay ($A_o = A_r = 100 \times 100$ km^2, $\lambda = 0.30$ km^{-1} and $D_{min} = 2$ km), N = 156 and the rain cell peak values R_G vary from $R_{G,1} = 168.95$ mm h^{-1} to $R_{G,156} = 1.02$ mm h^{-1}.

[32] From (10), the number of cells n_D whose diameter D at $R_2 = 1$ mm h^{-1} lies between D and D + ΔD over A_o is:

$$n_D(R_2) = \frac{4}{\lambda\pi}\left[\frac{D_{min}^2}{\lambda} + \frac{2D_{min}}{\lambda^2} + \frac{2}{\lambda^3}\right]^{-1} e^{\lambda D_{min}} P_r(R_2) \cdot \left[e^{-\lambda D} - e^{-\lambda(D+\Delta D)}\right] A_r. \quad (12)$$

[33] As for n_p, an over sampling ($D_{min} \leq D \leq 30$ km, $\Delta D = 0.001$ km) is first operated, followed by a resampling of D to finally obtain N values of D, $(D_i)_{i=1..N}$, sorted in descending order ($D_1 > D_2 > \ldots > D_N$), giving the diameter at 1 mm h^{-1} of the N hybrid cells filling A_o. Here, the maximum value of D, that is D_1, is not 30 km but is adjusted so as to comply optimally with the spatial requirement (3):

$$\sum_{i=1}^{N} \pi \frac{D_i^2(R_2)}{4} = A_r P(R \geq R_2 / R > R_r). \quad (13)$$

[34] Proceeding that way for Bombay ($A_o = A_r = 100 \times 100$ km^2, $\lambda = 0.30$ km^{-1}, $D_{min} = 2$ km) the N = 156 hybrid cells occupying A_o have a diameter at $R_2 = 1$ mm h^{-1} varying from $D_1 = 19.54$ km to $D_{156} = 2.01$ km.

[35] Now, one can wonder whether a relationship exists between the rain rate peak value of a cell and its area at 1 mm h^{-1}. To answer this question, from the database of Bordeaux and Karlsruhe [e.g., *Féral et al.*, 2003], the mean value of the rain cell area has been computed as a function of its peak intensity. From Figures 6 and 7, which correspond to the radar observations at Bordeaux and Karlsruhe, respectively, it appears that, in average, the rain cell area at 1 mm h^{-1} is a growing function of its peak rain rate. Nevertheless, this statistical result has to be handled with care. The common experience shows that a cell extracted from a rainy event of stratiform nature (wintry rain) can have an area at 1 mm h^{-1} several times greater than that of a convective cell identified in a summer storm at the same threshold. Now, when considering an observation area at a given time, the rain field will be either of stratiform or convective kind so that, as part of a scene generating, it is reasonable to assume that the cell having a peak intensity of 168.95 mm h^{-1} will occupy the greatest area at 1 mm h^{-1}, due to its spreading down to the lowest rain rate values. This leads to defining a bijective relationship between the peak values of the N hybrid cells filling A_o, $(R_{G,i})_{i=1..N}$, and the values of their diameter at 1 mm h^{-1} $(D_i)_{i=1..N}$ so that $R_{G,1}$ and D_1 refer to the first cell, $R_{G,2}$ and D_2 to the second one and so and so forth.

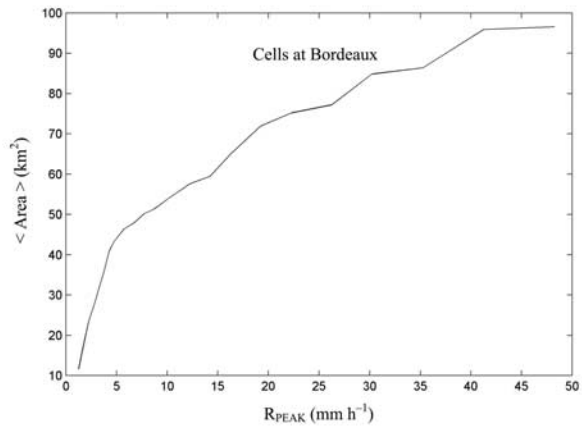

Figure 6. Mean value of the rain cell area <Area> at 1 mm h^{-1} as a function of their peak intensity R_{PEAK} from the radar observations at Bordeaux.

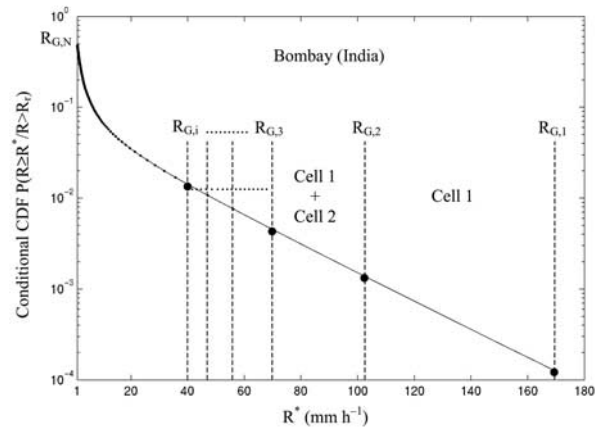

Figure 8. Conditional CDF $P(R \geq R^*/R > R_r)$ for Bombay (full line) and interpolated values (dots) at each of the peaks $(R_{G,i})_{i=1..N}$ of the N = 156 hybrid cells filling the observation area A_o of 100 × 100 km^2 (D_{min} = 2 km).

[36] At this stage, N hybrid cells are known to occupy the observation area A_o. Moreover, for each of them, the peak rain rate $(R_{G,i})_{i=1..N}$ and the diameter at 1 mm h^{-1} $(D_i)_{i=1..N}$ have been determined. In the next subsection, the parameters $(a_{G,i}, R_{1,i}, R_{E,i}, a_{E,i})_{i=1..N}$ missing for a full characterization of the N hybrid cells will be computed numerically, from the HYCELL model definition (1), under the constraint of accounting for the local CDF characteristic of the simulation area A_o.

4.2. Numerical Determination of $(a_{G,i}, R_{1,i}, R_{E,i}, a_{E,i})_{i=1..N}$

[37] One of the basic requirements of the scene that is being generated is to accurately reproduce the local CDF of the rain rate given by recommendation *ITU* [2001], on the definition domain of the HYCELL model, that is for $R \geq R_2$, where R_2 = 1 mm h^{-1}. With this aim in view, the interpolated values of the conditional CDF, $P(R \geq R^*/R > R_r)$ are computed, for each of the peak values of the N hybrid cells filling A_o, that is for $(R_{G,i})_{i=1..N}$ with $R_{G,1} > R_{G,2} > \ldots > R_{G,N}$. The result is shown in Figure 8 for Bombay. From that figure, it appears that the whole information related to $P(R \geq R_{G,2}/R > R_r)$ comes from the first cell (the one whose peak value $R_G = R_{G,1}$ is the largest), the whole information related to $P(R \geq R_{G,3}/R > R_r)$ comes from the 1st and 2nd cells, and so on and so forth. This remark suggests the iterative determination of all the missing parameters to fully describe the N hybrid cells filling A_o. In such a way, from (1), the area A_1 of the 1st cell over which the rain rate exceeds $R_{G,2}$ is given by:

$$\left.\begin{aligned} A_1\left(R \geq R_{G,2}\right) &= \pi a_{G,1}^2 \ln\frac{R_{G,1}}{R_{G,2}} \quad \text{if } R_{G,2} \geq R_{1,1}, \\ &= \pi a_{E,1}^2 \ln^2\frac{R_{E,1}}{R_{G,2}} \quad \text{if } R_{G,2} < R_{1,1}, \end{aligned}\right\} \quad (14)$$

and from (3):

$$A_1\left(R \geq R_{G,2}\right) = P\left(R \geq R_{G,2}/R > R_r\right)A_r. \quad (15)$$

[38] Due to the bijective relationship between $(R_{G,i})_{i=1..N}$ and $(D_i)_{i=1..N}$, the diameter of the 1st hybrid cell at R_2 = 1 mm h^{-1}, D_1, can be related to its theoretical expression:

$$\left.\begin{aligned} D_1 &= 2a_{E,1}\ln\frac{R_{E,1}}{R_2} \quad \text{if } R_{1,1} > R_2 \\ &= 2a_{G,1}\ln^{1/2}\frac{R_{G,1}}{R_2} \quad \text{if } R_{1,1} = R_2 \end{aligned}\right\} \quad (16)$$

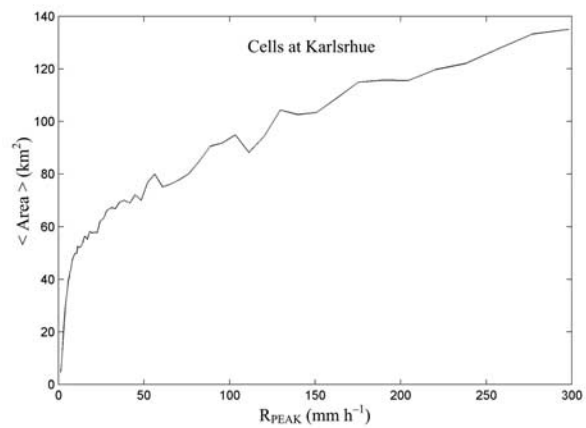

Figure 7. Same as Figure 6 but now from the radar observations at Karlsrhue.

[39] Moreover, it has been shown that, in the case of a HYCELL modeling, the conditional mean value of R_1 is 0.55 R_G so that $(R_{1,i})_{i=1..N}$ may be determined, a priori, for the N hybrid cells filling A_o from their peak values $(R_{G,i})_{i=1..N}$ previously obtained.

[40] And lastly, as mentioned by *Féral et al.* [2003], the HYCELL model verifies two continuity equations for $R = R_1$, which in the case of circular cells ($b_G = a_G$, $b_E = a_E$) reduce to:

$$a_E^2 \ln^2 \frac{R_E}{R_1} = a_G^2 \ln \frac{R_G}{R_1}. \tag{17}$$

[41] Therefore, from the above equations, the 1st cell filling the observation area A_o is fully determined by resolving the system of 3 equations with 3 unknowns ($a_{G,1}$, $R_{E,1}$, $a_{E,1}$):

$$\left.\begin{aligned} P\left(R \geq R_{G,2}/R > R_r\right)A_r &= \pi a_{G,1}^2 \ln \frac{R_{G,1}}{R_{G,2}} \quad \text{if } R_{G,2} \geq R_{1,1}, \\ &= \pi a_{E,1}^2 \ln^2 \frac{R_{E,1}}{R_{G,2}} \quad \text{if } R_{G,2} < R_{1,1}, \end{aligned}\right\} \tag{18}$$

$$\left.\begin{aligned} D_1 &= 2a_{E,1} \ln \frac{R_{E,1}}{R_2} \quad \text{if } R_{1,1} > R_2, \\ &= 2a_{G,1} \ln^{1/2} \frac{R_{G,1}}{R_2} \quad \text{if } R_{1,1} = R_2, \end{aligned}\right\} \tag{19}$$

$$a_{E,1}^2 \ln^2 \frac{R_{E,1}}{R_{1,1}} = a_{G,1}^2 \ln \frac{R_{G,1}}{R_{1,1}} \tag{20}$$

[42] At the second iteration, when considering the area A_2 of the 2nd cell over which the rain rate exceeds $R_{G,3}$, (15) becomes:

$$A_2\left(R \geq R_{G,3}\right) = P\left(R \geq R_{G,3}/R > R_r\right)A_r - A_1\left(R \geq R_{G,3}\right) \tag{21}$$

in which the contribution of the 1st cell, that is $A_1(R \geq R_{G,3})$, is computed from its HYCELL modeling whose parameters ($R_{G,1}$, $a_{G,1}$, $R_{E,1}$, $a_{E,1}$, $R_{1,1}$) are now fully determined.

[43] Finally, at the ith iteration, the determination of the parameters ($a_{G,i}$, $R_{E,i}$, $a_{E,i}$) of the ith cell requires the resolution of the system:

$$\left.\begin{aligned} A_i\left(R \geq R_{G,i+1}\right) &= \pi a_{G,i}^2 \ln \frac{R_{G,i}}{R_{G,i+1}} \quad \text{if } R_{G,i+1} \geq R_{1,i} \\ &= \pi a_{E,i}^2 \ln^2 \frac{R_{E,i}}{R_{G,i+1}} \quad \text{if } R_{G,i+1} < R_{1,i} \end{aligned}\right\} \tag{22}$$

$$\left.\begin{aligned} D_i &= 2a_{E,i} \ln \frac{R_{E,i}}{R_2} \quad \text{if } R_{1,i} > R_2, \\ &= 2a_{G,i} \ln^{1/2} \frac{R_{G,i}}{R_2} \quad \text{if } R_{1,i} = R_2, \end{aligned}\right\} \tag{23}$$

$$a_{E,i}^2 \ln^2 \frac{R_{E,i}}{R_{1,i}} = a_{G,i}^2 \ln \frac{R_{G,i}}{R_{1,i}}, \tag{24}$$

where

$$A_i\left(R \geq R_{G,i+1}\right) = P\left(R \geq R_{G,i+1}/R > R_r\right)A_r - \sum_{j=1}^{i-1} A_j\left(R \geq R_{G,i+1}\right). \tag{25}$$

Thus, the missing parameters ($a_{G,i}$, $R_{E,i}$, $a_{E,i}$)$_{i=1..N}$ to fully describe the N hybrid cells filling A_o are determined cell after cell, by means of an iterative process, starting from those whose peak values R_G are the largest.

[44] Obviously, insofar as $R_1 = 0.55\ R_G$ is imposed, this methodology would be able to generate only hybrid cells ($R_2 < R_1 < R_G$) whenever $R_G > (R_2/0.55)$. Now, as shown by *Féral et al.* [2003], rain fields are also composed of purely gaussian ($R_1 = R_2$) and purely exponential ($R_1 = R_E = R_G$) cells. This would require a correction of $(R_{1,i})_{i=1..N}$. The next subsection shows that the latter is necessary, from a purely numerical point of view, to accurately reproduce the local CDF P_r.

4.3. Iterative Correction of $(R_{1,i})_{i=1..N}$

[45] As previously mentioned, in the foregoing, R_1 has been attributed its conditional mean value with respect to R_G, that is $R_1 = 0.55\ R_G$. This hypothesis, though statistically correct (see Section 2.1), does not allow, on a purely numerical point of view, to produce a rain rate field which, at each step of its iterative generation, accurately agrees with the local CDF.

[46] Indeed, at the ith iteration, that is when determining the ith cell of peak $R_{G,i}$, the whole information related to $P(R \geq R_{G,i+1}/R > R_r)$ can be produced by the (i-1) hybrid cells that have already been generated over A_o. In other words, according to (25):

$$\sum_{j=1}^{i-1} A_j\left(R \geq R_{G,i+1}\right) > P\left(R \geq R_{G,i+1}/R > R_r\right)A_r, \tag{26}$$

where $A_j(R \geq R_{G,i+1})$ is the area of the jth cell already generated, over which the rain rate exceeds $R_{G,i+1}$.

[47] This point can be overcome by correcting R_1 by means of an iterative process. Indeed, at each iteration i, the additional hybrid cell of peak $R_{G,i}$ to be determined has to occupy the whole area A_i which is

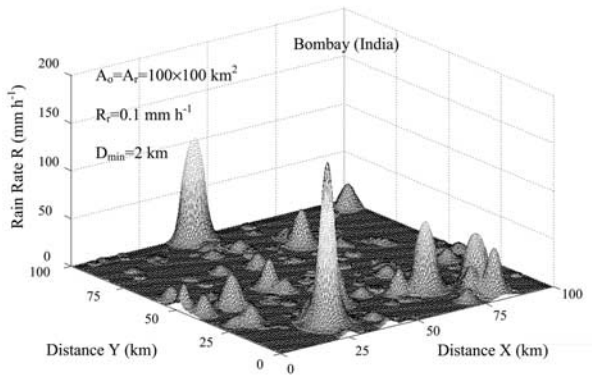

Figure 9. Statistical modeling of a rain field in the region of Bombay, India ($A_o = A_r = 100 \times 100$ km^2, $R_r = 0.1$ mm h^{-1}, $D_{min} = 2$ km).

assigned at $R_{G,i+1}$ by (25), while its contribution at $R_{G,i+2}$ must not represent the whole information available, that is:

$$A_i\left(R \geq R_{G,i+2}\right) + \sum_{j=1}^{i-1} A_j\left(R \geq R_{G,i+2}\right) < P\left(R \geq R_{G,i+2}/R > R_r\right)A_r \qquad (27)$$

[48] This condition allows to control the value of $R_{1,i}$ to insure the existence of the next cell of peak $R_{G,i+1}$. $R_{1,i}$ can thus take all the values from $R_{G,i}$ down to $R_2 = 1$ mm h^{-1}. The cell distribution $n_p(R_G)$ is thus rigorously respected and the error with respect to the conditional CDF $P(R \geq R_{G,i+1}/R > R_r)$ is minimized. Therefore, the rain field generated has a mixed composition of cells: hybrid ($R_2 < R_1 < R_G$, with R_1 equal to its mean value whenever (27) is verified), purely gaussian ($R_1 = R_2$), and purely exponential ($R_1 = R_E = R_G$).

[49] Figure 9 shows the two-dimensional rain field obtained that way for Bombay ($A_o = A_r = 100 \times 100$ km^2, $\lambda = 0.30$ km^{-1} and $D_{min} = 2$ km), the rain cell location being determined from a random number generator. In that case, among the 156 cells generated over A_o, 126 are hybrid, 3 purely gaussian, and 27 purely exponential. As previously mentioned, their peak rain rate varies from 1.02 to 168.95 mm h^{-1}, while their diameter at 1 mm h^{-1} varies from 2.01 km to 19.54 km.

[50] Figure 10 shows the conditional CDFs $P(R \geq R^*/R > R_r)$ at Bombay derived from recommendation *ITU* [2001] and computed from the scene shown in Figure 9, over the probability range from 10^{-3} to 1. If the N hybrid cells filling A_o are parameterized, at each step of their iterative generation, by minimizing the error with respect to the local CDF, the values considered for R during the minimization process are still limited to the values $(R_{G,i})_{i=2..N}$, defining a discrete number of test values. Nevertheless, Figure 10 leads to the observation that for all R, from 1 up to 110 mm h^{-1}, the two CDF coincide very well. So as to quantitatively assess the ability of the simulated scenes to reproduce the rain rate distribution, the mean $\bar{\xi}$, standard deviation ξ_{std}, and root mean square ξ_{rms} values of the relative error ξ, with respect to R between the conditional CDF derived from recommendation *ITU* [2001], and the one derived from the simulated scene, have been computed, for the "standard" probabilities 0.001, 0.002, 0.003, 0.005, 0.01, 0.02, 0.03, 0.05, 0.1, 0.2, 0.3, 0.5. This error criterion is defined by *Poiares-Baptista and Salonen* [1998]. The results are shown in Table 2. For Bombay, the mean and rms values of the relative error on the local CDF are 1.21% and 2.22%, respectively, confirming the ability of the generated scene to account for the local climatology.

[51] Consequently, the iterative correction of R_1, which originates from purely calculatory considerations, still allows all the potentialities of the HYCELL model to be used in order to generate a scene whose CDF accurately reproduces the local CDF given as an input parameter. Moreover, this iterative correction allows to account, to a certain extent, for the variabilities of parameter R_1 reported in Section 2.1. The HYCELL modeling of rain cells combined with the above methodology then allows the statistical modeling of the rain rate field horizontal structure while respecting the local climatology.

4.4. Examples of Scenes Generated

[52] Various scenes of rainy events have been simulated over observation areas with different climatologies to evaluate the ability of the "hybrid" methodology ("hybrid" because using the hybrid model HYCELL)

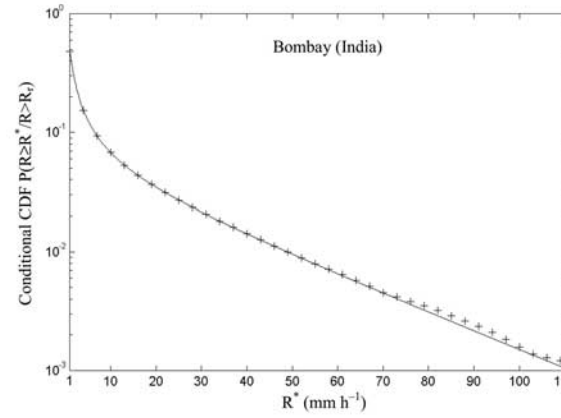

Figure 10. Conditional CDF $P(R \geq R^*/R > R_r)$ for Bombay derived from recommendation *ITU* [2001] (full line) and conditional CDF computed from the generated scene shown in Figure 9 (crosses).

Table 2. Mean $\overline{\xi}$, Standard Deviation ξ_{std}, and Root Mean Square ξ_{rms} of the Relative Error ξ With Respect to R Between the Conditional CDFs Derived From Recommendation *ITU* [2001] and Derived From the Simulated Scenes, for the "Standard" Probabilities 0.001, 0.002, 0.003, 0.005, 0.01, 0.02, 0.03, 0.05, 0.1, 0.2, 0.3, 0.5

	Bombay	Bordeaux	Pointe-à Pitre	Madras	Jakarta	Cayenne	Moscow	Glasgow	Global
$\overline{\xi}$	1.21%	0.49%	1.46%	0.82%	1.81%	1.25%	1.86%	0.70%	1.20%
ξ_{std}	1.87%	0.66%	2.07%	1.46%	3.20%	2.01%	4.28%	1.07%	2.39%
ξ_{rms}	2.22%	0.82%	2.53%	1.67%	3.67%	2.36%	4.66%	1.27%	2.67%

to account for the local CDF. Figure 11 results from the statistical modeling of the rain field in the region of Bordeaux (l = 44°49′N, L = 0°42′E, southwestern France, midlatitude oceanic climate). In that case, 138 cells are generated over A_o. 123 are hybrid, 11 purely gaussian, and 4 purely exponential. As Figure 10, Figure 12 shows the conditional CDFs $P(R \geq R^*/R > R_r)$ of Bordeaux derived from recommendation *ITU* [2001] and computed from the scene generated in Figure 11. Figure 12 underlines the ability of capturing the local CDF using the simulated scene. Table 2 shows that the relative error with respect to the local CDF is smaller than that for Bombay. Indeed, whatever the $\overline{\xi}$ or ξ_{rms} considered, the relative error remains below 1%.

[53] Figures 13a–13f refer to the statistical modeling of rain field in the regions of Pointe à Pitre (l = 16°15′ N, L = 61°30′ W, Guadeloupe, French West Indies, oceanic area of tropical climate), Madras (l = 13°00′ N, L = 80°10′ E, India, tropical climate with monsoon system), Jakarta (l = 6°06′ S, L = 106°39′ E, Malaysia, oceanic area of equatorial climate), Cayenne (l = 4°49′ N, L = 52°21′ W, French Guyana, oceanic area of equatorial climate), Moscow (l = 55°45′ N, L = 37°33′ E, Russia, midlatitude continental climate), and Glasgow (l = 55°51′ N, L = 4°25′ W, Scotland, midlatitude oceanic climate), respectively. From Table 2, it appears that the mean error $\overline{\xi}$ with respect to the local CDF is always lower than 1.86% whatever the location, that is whatever the climatology. Moreover, still from Table 2, when considering together the 8 locations, the mean, std, and rms values of the relative error are $\overline{\xi}$ = 1.20%, ξ_{std} = 2.39% and ξ_{rms} = 2.67%, respectively. These results demonstrate self consistency to the hybrid methodology as for its ability to generate two-dimensional rain rate fields throughout the world while accounting for the local CDF.

[54] In all these figures, the rain cell location is determined from a random number generator. In the case of real rain fields, the cells may cluster. For example, in tropical regions, rain cells are frequently organized in "squall lines", in which heavy rain cells are confined to a narrow convective line followed by a wide stratiform area [e.g., *Nzeukou and Sauvageot*, 2002]. It would then be necessary for the last step of the process to subsequently reorganize the generated field to make it more realistic. So as to account for the internal organization of rain fields, parameters such as the intercellular distance would prove very interesting. Moreover, rain cells do not have a perfectly smooth contour, which would result in a low value of the fractal dimension (∼1). Indeed, *Féral and Sauvageot* [2002] have shown that the fractal dimension of ordinary convective cells, when approached by the Hausdorff dimension, is close to 1.30. A solution could then be to deface the contour of the cells, by noising the field, until their fractal dimension becomes close to 1.30 while respecting the rain rate distribution.

4.5. Elliptic Rain Cells

[55] In the foregoing, the cells were assumed to be of circular shape. As part of an elliptic approach, *Féral et al.* [2000] have shown that the rain cell minor axis distribution (RCmAD) can be represented by a power law. Now, an exponential form is also convenient so that:

$$N(m, \tau) = N_1(\tau) \exp[-\beta(\tau)m] \qquad (28)$$

where m is the minor axis length and τ the threshold. $N(m, \tau)$ is the number of cells having a minor axis m, per unit area, inside an observed area A_o, and $N_1(\tau)$ and $\beta(\tau)$ are the two parameters of the distribution, that is the intercept and the slope, respectively. As $N(D, \tau)$, $N(m, \tau)$

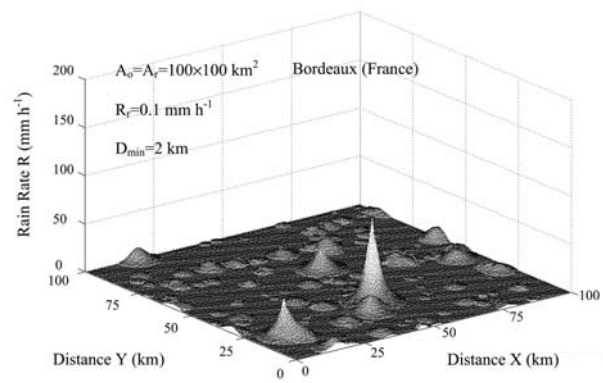

Figure 11. Statistical modeling of a rain field in the region of Bordeaux, southwestern France, midlatitude oceanic climate ($A_o = A_r = 100 \times 100$ km^2, R_r = 0.1 mm h^{-1}, D_{min} = 2 km).

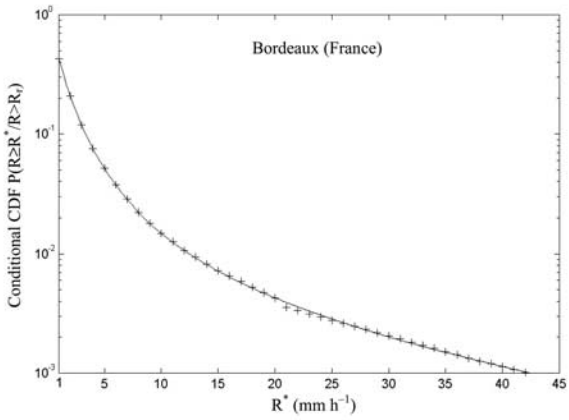

Figure 12. Conditional CDF $P(R \geq R^*/R > R_r)$ for Bordeaux (southwestern France) derived from recommendation *ITU* [2001] (full line) and computed from the generated scene shown in Figure 11 (crosses).

has to be understood as being the minor axis distribution given it is raining over A_o.

[56] From the radar data at Bordeaux and Karlsruhe [*Féral et al.*, 2003], the RCmAD has been computed. Results primarily show that, for the cells at Bordeaux as for those at Karlsruhe, the slope β is weakly dependent on the threshold τ and $\beta(\tau) = \beta = 0.35$ km^{-1}. Though these two locations differ from the climatic context, oceanic for Bordeaux and continental for Karlsruhe, they are both situated at midlatitude so that one cannot conclude that $\beta = 0.35$ km^{-1} is a climatic constant: the study has to be extended to places with different climatologies.

[57] Nevertheless, if it is assumed that β is a climatic constant and that the majority of the cells are twice longer than wide [*Pawlina and Binaghi*, 1995; *Féral et al.*, 2000], it then becomes possible to generate two-dimensional rain fields composed of hybrid cells of elliptic horizontal cross section.

[58] Indeed, as part of the HYCELL modeling, the last assumption leads to considering that $b_E = 2a_E$ and $b_G = 2a_G$. Considering the exponential form (28) to represent the rain cell minor axis distribution, the expressions of the cell density N_P (spatial density per value of R_G) and N_m (spatial density per value of m) can be derived so that the whole methodology previously presented can be applied to the scene synthesis obtained from hybrid cells of elliptic shape.

5. Comparison With Another Method

5.1. Methodology of Goldhirsh

[59] The methodology developed by *Goldhirsh* [2000] to generate two-dimensional rain rate fields lies on the description of the rain rate horizontal distribution within the cells by the EXCELL model [*Capsoni et al.*, 1987b]. Considering its monoaxial formulation, the analytical expression of the rain rate distribution within a cell is then given by:

$$R(r) = R_E \exp\left[-\left(\frac{r}{\rho_o}\right)\right], \text{for } R_E > R_{min} \tag{29}$$

In (29), R_E is the peak rain rate, r is the radial distance from the center of the cell and ρ_o is the radial distance for which R decreases by a factor 1/e with respect to R_E. The minimum rain rate value R_{min} defines the validity domain of EXCELL ($R \geq R_{min}$) which, in its primary formulation [*Capsoni et al.*, 1987b], is $R_{min} = 5$ mm h^{-1}.

[60] From 6215 radar cells identified at 5 mm h^{-1}, *Capsoni et al.* [1987b] showed empirically that the statistical average of ρ_o, that is $\overline{\rho_o}$, is given by:

$$\overline{\rho_o}(R_E) = 1.7\left[\left(\frac{R_E}{6}\right)^{-10} + \left(\frac{R_E}{6}\right)^{-0.26}\right], \quad \text{for } R_E > 5\text{mmh}^{-1}. \tag{30}$$

Now, (30) was derived from radar observations of rain field at Spino d' Adda, near Milan (Italy). Therefore, the validity of (30) in other parts of the world remains questionable.

[61] In other respects, *Awaka* [1989] extended the analysis of *Capsoni et al.* [1987b] for values down to $R_{min} = 0.4$ mm h^{-1} by assuming that:

$$\overline{\rho_o}(R_E) = \frac{10 - 1.5\log_{10} R_E}{\ln \frac{R_E}{0.4}}, \qquad \text{for } R_E > 0.4\text{h}^{-1}. \tag{31}$$

Equation (31) is of prime importance in the methodology of two-dimensional scene generating developed by *Goldhirsh* [2000]. Indeed, it allows to turn the monoaxial formulation of the EXCELL model, depending on two parameters (R_E, ρ_o), into a one parameter model (R_E). As part of a spatial generating of rain cells over a simulation area A_o, the key parameter is the cell spatial density. When the cells are fully described by a peak rain rate R_E, ρ_o coming from (30) or (31), the key point is then the determination of $N(R_E)$, that is the rain cell spatial density per value of R_E. *Capsoni et al.* [1987b] showed that a general retrieval algorithm for $N(R_E)$ is given by:

$$N(R_E) = -\left(\frac{1}{4\pi R_E \overline{\rho_o^2}(R_E)}\right) \frac{d^3 P(R > R^*/R > R_r)}{d(\ln R)^3}\Big|_{R=R_E} \tag{32}$$

Awaka [1989] derived an expression similar to (32) except for a factor of 2. As for (30) and as mentioned by

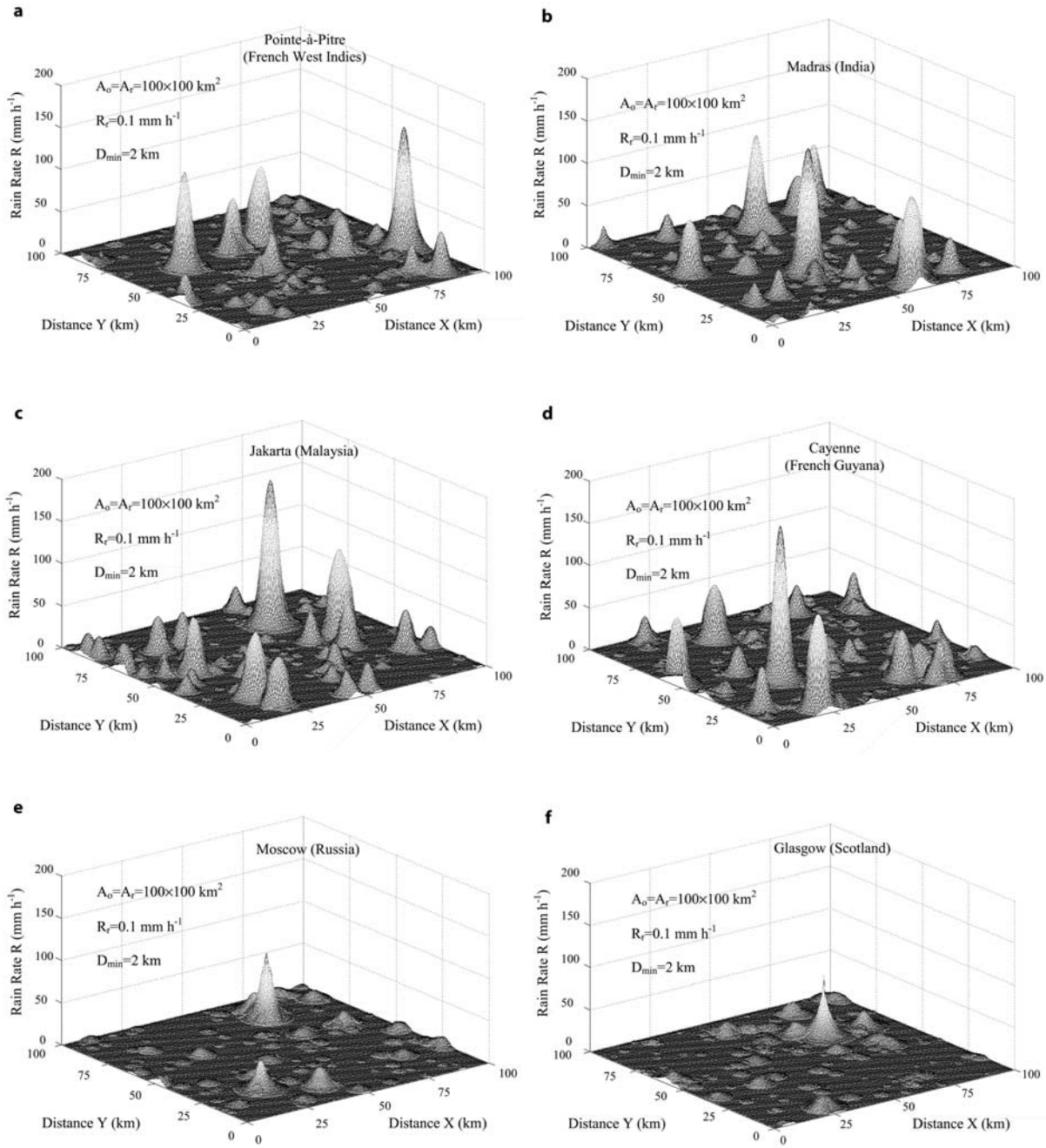

Figure 13. (a) Statistical modeling of a rain field in the region of Pointe-à-Pitre, Guadeloupe, French West Indies, oceanic area of tropical climate. (b) Statistical modeling of a rain field in the region of Madras, India, tropical climate with a monsoon system. (c) Statistical modeling of a rain field in the region of Jakarta, Malaysia, oceanic area of equatorial climate. (d) Statistical modeling of a rain field in the region of Cayenne, French Guyana, oceanic area of equatorial climate. (e) Statistical modeling of a rain field in the region of Moscow, Russia, midlatitude continental climate. (f) Statistical modeling of a rain field in the region of Glasgow, Scotland, midlatitude oceanic climate.

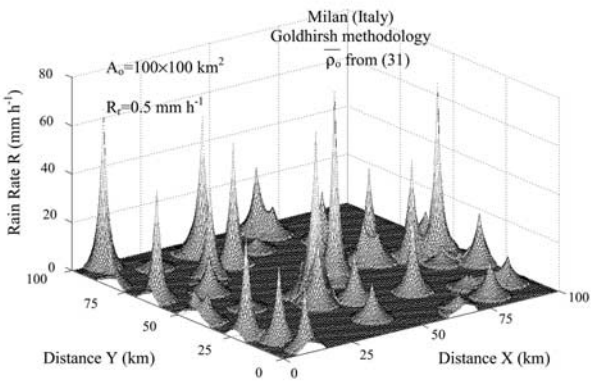

Figure 14. Statistical modeling of a rain field in the region of Milan, Italy (l = 45° N, L = 8°1′ E) using the *Goldhirsh* [2000] methodology, that is, when $\overline{\rho_o}$ in (32) takes the value $\overline{\rho_o}$ defined in (31) (*Awaka* [1989] hypothesis).

Goldhirsh [2000], (32) was derived by *Capsoni et al.* [1987b] from radar measurements in the region of Milan, so that the validity of (32) in other parts of the world is questionable.

[62] In (32), $P(R \geq R^*/R > R_r)$ is the conditional CDF P_r defined in section 3.2. The computation of the third derivative of P_r with respect to lnR would be facilitated by the use of an analytical approximation of P_r. In such a way, *Capsoni et al.* [1987a] proposed to approximate P_r by a function differentiable with respect to lnR, in the form:

$$P(R \geq R^*/R > R_r) = P_o \ln^{\kappa}(R_M/R^*) \qquad (33)$$

Now, the analytical approximation of the conditional CDF P_r by (33) may introduce errors.

5.2. Comparison With the Hybrid Methodology

[63] Following the step by step methodology developed by *Goldhirsh* [2000], the two-dimensional generating of a rain field in the region of Milan has been operated (l = 45° N, L = 8°1′ E). Insofar as the region of Milan is the place where (30) and (32) were established, the choice of this location constitutes, a priori, a ''best place design'' for using the methodology of Goldhirsh and the results of *Capsoni et al.* [1987b]. The observation area A_o is still 100 × 100 km^2 while the threshold condition of rain R_r is now 0.5 mm h^{-1}, in compliance with *Goldhirsh* [2000]. Applying a curve fitting routine to the conditional CDF derived from recommendation *ITU* [2001], the parameters of the analytical approximation of $P(R \geq R^*/R > R_r)$ by (33) are found to be Po = 5.0035 × 10^{-5}, κ = 5.28, R_M = 340 mm h^{-1}, with a rms rain rate deviation, as defined by Goldhirsh, equal to 1.19 mm h^{-1}, a value comparable to the rms deviations reported by *Goldhirsh* [2000].

[64] Figure 14 shows the two-dimensional scene generated from the methodology of *Goldhirsh* [2000], that is when $\overline{\rho_o}$ in (32) takes the value $\overline{\rho_o}$ defined in (31) (assumption of *Awaka* [1989]), and when (32) is multiplied by a factor of two. Here, in compliance with *Goldhirsh* [2000], R_E varies from 2.5 mm h^{-1} to R_M by 5 mm h^{-1} steps. The cell contribution is extended down to $R = R_2 = 1$ mm h^{-1}. The number of cells generated that way over A_o is equal to 46. The rain cell location is determined from a random number generator. Besides, so as to compare the number of cells generated over A_o, the methodology of Goldhirsh has been implemented with the results of *Capsoni et al.* [1987b], that is when $\overline{\rho_o}$ in (32) takes the value specific to the region of Milan defined by (30). To comply with the domain of definition of (30), R_E now varies from 5 mm h^{-1} to R_M by 5 mm h^{-1} steps. The total number of cells occupying A_o is then equal to 44.

[65] The two-dimensional scene generating for Milan from hybrid cells has been operated, following the hybrid methodology developed in section 4 ($A_o = A_r = 100 \times 100$ km^2, $R_2 = 1$ mm h^{-1} with now $R_r = 0.5$ mm h^{-1}). Equation (32) was obtained by *Capsoni et al.* [1987b] assuming that ρ_o varies from 0 to ∞. As part of a scene generation from the hybrid methodology, it leads to considering that D_{min} is equal to 0 km. Of course it is not reasonable to consider cells with such small dimensions. First, because in nature, cells with size below a few hundred meters would not be sufficiently persistent to develop a reflectivity core identifiable as a rain cell, even at low rain rate values. Indeed, *Benner and Curry* [1998] pointed out that clouds smaller than about one kilometer are not seen to precipitate. Secondly, and as mentioned in Section 2.2, the domain of validity of (2) is 2 km $\leq D \leq$ 20 km so that (2) is not valid down to a few meters. Thus, the value D_{min} = 0 km is used here only for comparison's sake. The simulated rain field is shown in Figure 15. The rain cell location is determined from a random number generator. The number of cells whose peak rain rate is greater than 5 mm h^{-1} is 44, that is exactly the value obtained from the methodology of Goldhirsh implemented with the results of *Capsoni et al.* [1987b]. Now, for the case of the hybrid methodology, the rain cell spatial density as given by (9) does not refer to any site specific parameter as $\overline{\rho_o}$ in (31) or (32), but to a widely studied distribution in various latitudes, namely the rain cell diameter distribution.

[66] Figure 16 shows the conditional CDF $P(R \geq R^*/R > R_r)$ of Milan as well as those computed from the scenes shown in Figures 14 and 15. Unlike the scene simulated from the hybrid methodology, the rain field generated from the methodology of Goldhirsh does not represent as accurately the local CDF. Indeed, from a quantitative

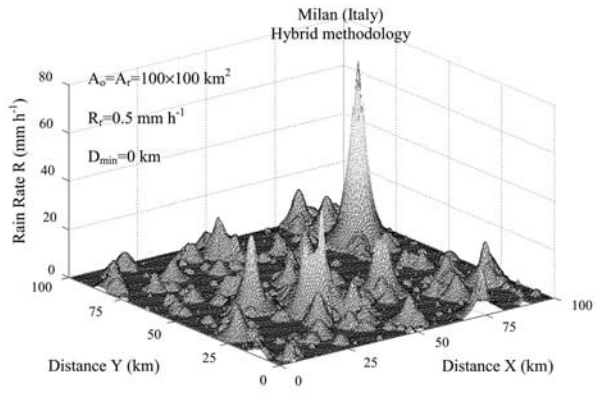

Figure 15. Statistical modeling of a rain field in the region of Milan, Italy (l = 45° N, L = 8°1′ E) using the hybrid methodology. $A_o = A_r = 100 \times 100$ km^2, $R_r = 0.5$ mm h^{-1}, $D_{min} = 0$ km.

point of view, the mean, std, and rms values of the relative error ξ defined in Section 4.3 are $\overline{\xi} = 13.42\%$, $\xi_{std} = 6.71\%$, and $\xi_{rms} = 15.01\%$, respectively, for the scene simulated using the methodology of Goldhirsh. When considering the scene generated according to the hybrid scheme, these values become $\overline{\xi} = 0.64\%$, $\xi_{std} = 0.94\%$, and $\xi_{rms} = 1.14\%$. The improvement is clear. Now, this result should not be a surprise insofar as the cells are not parameterized iteratively, to comply accurately with the successive values of the local CDF, but are fully described by (32) which refers only to the rain cell spatial density per value of R_E.

6. Conclusion

[67] A methodology to generate typical two-dimensional rain rate fields throughout the world has been presented. The simulated rain fields account for the climatological characteristics associated with the simulation area A_o.

[68] The rain field is assumed to result from the conglomeration of rain cells. The methodology lies on the description of the rain cell horizontal structure by the HYCELL model. Therefore, the modeling of a rain cell requires the determination of seven parameters, namely R_G, a_G, b_G, R_E, a_E, b_E, and R_1. $\{R_G, a_G, b_G\}$ and $\{R_E, a_E, b_E\}$ define the gaussian and exponential components, respectively, while R_1 delimits the zones of gaussian and exponential definition. Considering rain cells of circular horizontal cross section, the number of parameters reduces to five (R_G, a_G, R_E, a_E, and R_1) insofar as $a_G = b_G$ and $a_E = b_E$. Now, from the HYCELL modeling of more than 900,000 rain cells, it was shown, from a statistical point of view, that the conditional mean value of R_1 given R_G is very close to 0.55 R_G.

[69] As part of a two-dimensional scene generating over an observation area A_o from a population of (circular) cells modeled by HYCELL, the key parameter is the rain cell spatial density. Two analytical expressions have been derived for the latter, both involving the local CDF characteristic of the simulation area A_o. They both result from the rain cell size distribution (RCSD), which was shown by many authors and in various latitudes to be well represented by an exponential form, with a slope λ weakly dependent on the geographical location.

[70] Now, from the two analytical expressions of the rain cell spatial density, the number N of hybrid cells occupying A_o, their peak value $(R_{G,i})_{i=1..N}$ and diameter at 1 mm h^{-1} $(D_i)_{i=1..N}$ can be determined. Moreover, using the HYCELL model definition and the ergodic character of precipitation fields, the four parameters $(a_{G,i}, R_{E,i}, a_{E,i}, R_{1,i})_{i=1..N}$ missing to fully characterize the N hybrid cells filling A_o are computed, cell after cell, by means of an iterative process, with the constraint of accurately reproducing the local CDF. This requirement results in the iterative correction of R_1, which can finally take all the values from R_G down to 1 mm h^{-1}. Therefore, the rain field generated has a mixed composition of hybrid ($R_2 < R_1 < R_G$), purely gaussian ($R_1 = R_2$) and purely exponential cells ($R_1 = R_E = R_G$), thus using all the potentialities of the HYCELL model to simulate a scene whose CDF accurately reproduces the local CDF given as an input parameter.

[71] So as to evaluate the ability of the hybrid methodology to generate rain fields which account for the

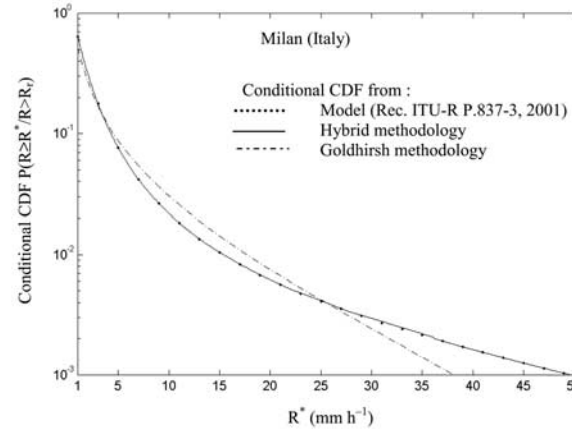

Figure 16. Conditional CDF $P(R \geq R^*/R > R_r)$ at Milan derived from recommendation *ITU* [2001] (dotted line), conditional CDF computed from the scenes shown in Figure 14 (dashed dotted line) and Figure 15 (full line). $A_o = A_r = 100 \times 100$ km^2, $R_r = 0.5$ mm h^{-1}.

local CDF, various scenes of rainy events have been simulated over observation areas of different climatologies. Considering the error criterion defined by *Poiares-Baptista and Salonen* [1998], namely, the relative error ξ with respect to R for conditional probabilities between 0.001 and 1, the results show that the mean value of ξ remains below 1.86% whereas the standard deviation remains lower than 4.28%, whatever the midlatitude, tropical, or equatorial region considered. In particular, a rain field has been generated in the region of Milan (Italy), using either hybrid or *Goldhirsh* [2000] methodology. The choice of Milan is not arbitrary insofar as this location is the place where most of the equations used by Goldhirsh were derived by *Capsoni et al.* [1987b]. The results show that the new methodology proposed reproduces the local CDF more accurately than the methodology of Goldhirsh, still without requiring any site-specific observation (other than the local CDF, of course).

[72] Consequently, the hybrid methodology of scene generating should be a powerful tool for system designers to evaluate at any location of the world, over an area of a few tens up to a few hundreds of square kilometers, representing the size of a satellite beam or a Broadband Wireless Access network (BWA), diversity gain, terrestrial path attenuation, or slant path attenuation for different azimuth directions, while accounting for the local climatological characteristics. Interference analysis and Fade Mitigation Techniques optimization for satellite communication systems would also benefit from this tool. Moreover, the hybrid methodology should be the starting point of a dynamic scene generating whenever a statistical description of the temporal evolution of the rain cell internal structure is available, from birth to decay, from the HYCELL parameters.

[73] Now, several simplifying assumptions that represent sources of errors must be kept in mind. Notably, the rain fields were generated over a simulation area A_o by assuming a conglomeration of rain cells modeled by HYCELL. Actual rain cells are significantly more complex, notably with respect to the horizontal cross section: cells do not have a perfectly smooth contour, which would result in a low value of the fractal dimension ($\sim$1). They rather show ragged and contorted contours, associated with a fractal dimension close to 1.30 [*Féral and Sauvageot*, 2002]. A procedure could be implemented to deface the cell contour, by introducing noise to the field until the rain cell fractal dimension becomes close to 1.30, while respecting the rain rate distribution. Besides, the rain cells were assumed to be uniformly distributed over A_o. An extension of the present work would consist in subsequently reorganizing the generated fields to make them more realistic. With this aim in view, so as to account for the internal organization of rain fields, parameters such as the intercellular distance would be very useful. Inputs coming from an analysis of large meteorological structures (frontal systems, squall line, etc.) would also be necessary for the larger scale, such as satellite beam. The validity of the generated scenes may also be partially checked by statistically modeling Earth-satellite paths through the modeled scenes and comparing the cumulative fade distribution obtained that way with the measured cases.

[74] **Acknowledgments.** The authors are very grateful to Météo-France and to Dr. Jan Handwerker, from the Institut für Meteorologie und Klimaforschung of Karlsruhe, for providing without fee the radar data from Bordeaux and Karlsruhe, respectively. They wish to thank Dr. Julius Goldhirsh for valuable comments and suggestions.

References

Awaka, J., A three-dimensional rain cell model for the study of interference due to hydrometeor scattering, *J. Commun. Res. Lab.*, *36*(147), 13–44, 1989.

Benner, T. C., and J. A. Curry, Characteristics of small tropical cumulus clouds and their impact on the environment, *J. Geophys. Res.*, *103*(D22), 28,753–28,767, 1998.

Bolea-Alamanac, A., and M. Bousquet, Millimetre-wave radio systems: Guidelines on propagation modelling and impairment mitigation techniques research needs, paper presented at First COST 280 Workshop, Malvern, UK, July 2002.

Capsoni, C., F. Fedi, and A. Paraboni, A comprehensive meteorologically oriented methodology for the prediction of wave propagation parameters in telecommunication applications beyond 10 GHz, *Radio Sci.*, *22*(3), 387–393, 1987a.

Capsoni, C., F. Fedi, C. Magistroni, A. Paraboni, and A. Pawlina, Data and theory for a new model of the horizontal structure of rain cells for propagation applications, *Radio Sci.*, *22*(3), 95–404, 1987b.

Castanet, L., J. Lemorton, and M. Bousquet, Fade mitigation techniques for new SatCom services at Ku-band and above: A review, paper presented at Fourth Ka-Band Utilization Conference, Venice, Italy, 2–4 Nov. 1998.

Castanet, L., J. Lemorton, T. Konefal, A. Shukla, P. Watson, and C. Wrench, Comparison of combined propagation models for predicting loss in low-availability systems that operate in the 20 GHz to 50 GHz frequency range, *Int. J. Satell. Commun.*, *19*(3), 317–334, 2001.

Castanet, L., D. Mertens, and M. Bousquet, Simulation of the performance of a Ka-band VSAT videoconferencing system with uplink power control and data rate reduction to mitigate atmospheric propagation effectsm, *Int. J. Satell. Commun.*, *20*(4), 231–249, 2002a.

Castanet, L., M. Bousquet, M. Filip, P. Gallois, B. Gremont, L. De Haro, J. Lemorton, A. Paraboni, and M. Schnell, Impairment mitigation and performance restoration, in *COST 255 Final Report*, *SP-1252*, chap. 5.3, Eur. Space Agency Publ. Div., Paris, March 2002b.

Dennis, A. S., and F. G. Fernald, Frequency distributions of shower sizes, *J. Appl. Meteorol.*, *2*, 767–769, 1963.

Drufuca, G., Radar-derived statistics on the structure of precipitation patterns, *J. Appl. Meteorol.*, *16*, 1029–1035, 1977.

Féral, L., and H. Sauvageot, Fractal identification of supercell storms, *Geophys. Res. Lett.*, *29*(14), doi:10.1029/2002GL015260, 2002.

Féral, L., F. Mesnard, H. Sauvageot, L. Castanet, and J. Lemorton, Rain cell shape and orientation distribution in South-West of France, *Phys. Chem. Earth B*, *25*(10–12), 1073–1078, 2000.

Féral, L., H. Sauvageot, L. Castanet, and J. Lemorton, HYCELL—A new hybrid model of the rain horizontal distribution for propagation studies: 1. Modeling of the rain cell, *Radio Sci.*, *38*, doi:10.1029/2002RS002802, in press, 2003.

Goldhirsh, J., Two-dimensional visualization of rain cell structures, *Radio Sci.*, *35*(3), 713–729, 2000.

Goldhirsh, J., and B. Musiani, Rain cell size statistics derived from radar observations at Wallops Island, Virginia, *IEEE Trans. Geosci. Remote Sens.*, *24*(6), 947–954, 1986.

International Telecommunication Union (ITU), Characteristics of precipitation for propagation modelling, vol. 2000, suppl. 1, P Ser., parts 1 and 2, *ITU-R Recomm. P 837-3*, Geneva, 2001.

Konrad, T. G., Statistical models of summer rain showers derived from fine-scale radar observations, *J. Appl. Meteorol.*, *17*, 171–188, 1978.

Lemorton, J., L. Castanet, V. Huot, and T. Marsault, A new opportunity for EHF propagation experiments: The EXPRESS campaign with the satellite STENTOR, *Int. J. Satell. Commun.*, *19*(3), 347–362, 2001.

Mesnard, F., and H. Sauvageot, Structural characteristics of rain fields, *J. Geophys.*, *108*, doi:10.1029/2002JD002808, in press, 2003.

Miller, J. R., A. S. Dennis, J. H. Hirsch, and D. E. Cain, Statistics of shower echoes in western North Dakota, paper presented at 16th Radar Meteorology Conference, Am. Meteorol. Soc., Houston, Tex., 1975.

Nzeukou, A., and H. Sauvageot, Distribution of rainfall parameters near the coast of France and Senegal, *J. Appl. Meteorol.*, *41*(1), 69–82, 2002.

Pawlina, A., and M. Binaghi, Radar rain intensity fields at ground level: New parameters for propagation impairments prediction in temperate regions, paper presented at 7th Commission F, Triennal Symposium, Union Radio Sci. Int., Ahmedabad, India, 1995.

Pech, P., M. Bousquet, L. Castanet, and J. Radzik, Insights into an architecture of Ka-band OBP satellite system involving FMTs, American Institute of Aeronautics and Astronautics Conference, Montreal, Que., Canada, May 2002.

Poiares-Baptista, J. P. V., and E.T. Salonen, Review of rainfall rate modelling and mapping, paper presented at Climpara'98, Ottawa, Ont., Canada, 1998.

Riva, C., Spatial characteristics of propagation parameters: A review, paper presented at First COST 280 Workshop, Malvern, UK, July 2002.

Sauvageot, H., F. Mesnard, and R. S. Tenorio, The relation between the area-average rain rate and the rain cell size distribution parameters, *J. Atmos. Sci.*, *56*, 57–70, 1999.

Silverman, B. W., *Density Estimation for Statistics and Data Analysis*, 175 pp., Chapman and Hall, New York, 1996.

Tenorio, R. S., H. Sauvageot, and S. Ramos-Buarque, Statistical studies of rain cell size distribution using radar data during squall line episodes in West Africa, paper presented at Third International Symposium on Hydrological Applications of Weather Radar, Sao Paulo, Brazil, 1995.

L. Castanet, L. Féral, and J. Lemorton, Département Electromagnétisme et Radar, ONERA, BP 4025, 2 avenue Edouard Belin, 31055 Toulouse Cedex 4, France. (laurent.feral@onera.fr)

H. Sauvageot, Observatoire Midi-Pyrénées, Laboratoire d'Aérologie, Université Paul Sabatier, 31400 Toulouse, France.